MOLECULAR AND CELLULAR BIOLOGY, Sept. 2007, p. 6396–6406 Vol. 27, No. 18
0270-7306/07/$08.00+0 doi:10.1128/MCB.00719-07

Replication in Hydroxyurea: It's a Matter of Time▽†

Gina M. Alvino,[1] David Collingwood,[2] John M. Murphy,[1] Jeffrey Delrow,[3] Bonita J. Brewer,[1] and M. K. Raghuraman[1]*

Department of Genome Sciences, University of Washington, Seattle, Washington 98195[1]; Department of Mathematics, University of Washington, Seattle, Washington 98195[2]; and Department of Genomic Resources, Fred Hutchinson Cancer Research Center, Seattle, Washington 98109[3]

Received 24 April 2007/Returned for modification 11 June 2007/Accepted 9 July 2007

Hydroxyurea (HU) is a DNA replication inhibitor that negatively affects both the elongation and initiation phases of replication and triggers the "intra-S phase checkpoint." Previous work with budding yeast has shown that, during a short exposure to HU, *MEC1*/*RAD53* prevent initiation at some late S phase origins. In this study, we have performed microarray experiments to follow the fate of all origins over an extended exposure to HU. We show that the genome-wide progression of DNA synthesis, including origin activation, follows the same pattern in the presence of HU as in its absence, although the time frames are very different. We find no evidence for a specific effect that excludes initiation from late origins. Rather, HU causes S phase to proceed in slow motion; all temporal classes of origins are affected, but the order in which they become active is maintained. We propose a revised model for the checkpoint response to HU that accounts for the continued but slowed pace of the temporal program of origin activation.

Eukaryotic genome duplication requires a complex coordination of successive events to initiate chromosome replication and distribute fully replicated chromosomes into the daughter cells. Chromosomal duplication is confined to the synthesis phase (S phase) of the cell cycle, where replication initiates from multiple specific sequences distributed along each chromosome called replication origins. Only a subset of all possible origins initiate synthesis in a given S phase, but these origins are activated in a temporal order that is, in general, conserved from one cell cycle to the next (24).

Surveillance mechanisms called checkpoints monitor chromosome duplication and respond to damage or defects by altering cellular metabolism in order to promote fidelity. In the absence of such safeguards, agents that challenge DNA synthesis by altering levels of necessary raw materials or by promoting damage could jeopardize chromosomal duplication and negatively affect the integrity of the genome. One such agent, hydroxyurea (HU), affects DNA synthesis by reversibly inhibiting ribonucleotide reductase (RNR), preventing the reduction of ribonucleotides to deoxyribonucleotides (deoxynucleoside triphosphates [dNTPs]). Unlike higher eukaryotes, wild-type *Saccharomyces cerevisiae* cells lack deoxyribonucleotide kinase activity and are therefore dependent upon RNR activity for dNTP production. The presence of high concentrations of HU (200 mM) prevents the accumulation of dNTPs that normally occurs as cells enter S phase (8, 21), impedes S phase progression, and engages the checkpoint to prohibit passage through the cell cycle into a catastrophic mitosis (reviewed in reference 28). In addition, wild-type cells activate transcription of genes involved in replication and repair (15, 18, 20) and stabilize the idling replication complex to allow the resumption of fork progression after the stress has been relieved (9, 23, 34, 35).

Nascent-strand analysis of wild-type cells replicating in the presence of HU failed to detect replication products from the late origin *ARS501* compared to the early origin *ARS305*, where such products were detected, suggesting that late origin activation is repressed in the presence of HU (1, 33). Electron micrographs of chromosomes from wild-type cells replicating in the presence of HU revealed bubble structures that contained obvious stretches of single-stranded DNA (ssDNA) but otherwise appeared normal (34). These replication bubbles expanded over time in HU, with forks advancing at a synthesis rate of ~50 bp minute^{-1} (34), a rate that is substantially lower than that estimated for unchallenged forks (31, 32). Since the molecules examined by electron microscopy were anonymous, the identities of the replicated regions were not known until Feng et al. used DNA microarrays to map the genomic locations of ssDNA that occur during HU treatment and confirmed that the sites that become single stranded early in HU treatment correspond to many of the more efficient and/or early-firing origins of replication (14).

Checkpoint-deficient cells undergoing HU treatment have been widely studied. The cellular and chromosomal responses to HU-induced replication stress have been shown to be dependent on the *MEC1*/*RAD53* checkpoint pathways (2, 9, 18, 23, 33, 35, 36). Electron micrographs of chromosomal DNA from a *rad53* mutant in HU revealed bubble structures that failed to expand into neighboring sequences over time and contained extensive regions of ssDNA, often encompassing one entire arm of the bubble (34). In *rad53* and *mec1* mutants, nascent DNA strand analysis detected products from both early and late origins by 90 min in HU (1, 33). The appearance of nascent strands at late origins in these checkpoint mutants led to the conclusion that late origins are specifically inactivated in wild-type cells by the *MEC1*/*RAD53* origin-firing checkpoint during HU-induced stress (33). However, even in

* Corresponding author. Mailing address: Department of Genome Sciences, University of Washington, Seattle, WA 98195. Phone: (206) 543-0334. Fax: (206) 685-7301. E-mail: raghu@u.washington.edu.

† Supplemental material for this article may be found at http://mcb.asm.org/.

▽ Published ahead of print on 16 June 2007.

these *rad53* and *mec1* mutants, nascent strands from an early origin still appeared earlier than those from a late origin (1, 33). Genome-wide analysis of ssDNA formation in *rad53* cells is consistent with this observation: the ssDNA loci that appear within 30 minutes after releasing *rad53* cells into HU are the same as the subset of origins that accumulate ssDNA in the wild-type culture undergoing HU treatment (14). Moreover, the origins that fail to accumulate ssDNA in wild-type cells become single stranded by 60 minutes in the *rad53* mutant (14). Because at least some temporal order of origin activation appears to be maintained in the *rad53* mutant in the presence of HU (1, 14, 33), it is clear that this checkpoint pathway can modulate the temporal program but is not involved in establishing it.

A feature common to many studies of origin firing in the presence of HU is the time interval over which replication is examined. In most cases it is equivalent to the approximate length of an untreated-cell cycle (90 to 120 min). However, in the presence of HU, wild-type cells may still be actively synthesizing DNA at the end of the collection period since flow cytometry shows that most cells have substantially less than a 2C DNA content (21, 22). The observation that origin firing is detected only at some origins in wild-type cells during the first 90 min in HU can be interpreted in two ways: (i) that, as proposed by Santocanale and Diffley (33), the *RAD53*-dependent checkpoint responds to HU by allowing firing of early-S origins while specifically preventing firing of late-S origins; or (ii) that, rather than acting at a particular class of origins, the *RAD53* checkpoint acts globally to slow down S phase progression and the rate of new origin initiations. Indeed, recent work on replication foci in *Schizosaccharomyces pombe* (25) is suggestive of continued S phase progression in the presence of HU, although the anonymity of replication foci and the incompletely characterized replication program in *S. pombe* left open the question of whether origin activations follow the normal pattern in the presence of HU.

In this study, we distinguish between the two models by following the S phase response to HU in wild-type cells over an extended length of time. We have used microarrays to measure the level of replication across the entire genome by analyzing samples collected at different times during S phase. By monitoring the kinetics of genome replication, we have identified which origins are activated in the presence and absence of the drug at different stages within these two very different S phases. As in previous studies, we see that only a small subset of origins is activated in HU early in S phase. However, we find that replication continues at a steady rate for at least 6 h, with additional origins becoming active during this interval. When we compared HU-treated and untreated samples that had attained similar levels of total genomic replication, regardless of the time required to attain that level of synthesis, we found remarkably similar patterns of origin activity, indicating that the temporal program is intact but executed at a much slower pace. Our findings support the hypothesis that, rather than specifically preventing late origin activation, the HU checkpoint acts by modulating the pace of the temporal program of activation of all origins in response to slowed fork rates and/or limiting dNTPs.

MATERIALS AND METHODS

Yeast strains and growth conditions. Yeast strain KK14-3a (*MAT***a** *cdc7-1 bar1 trp1-289 leu2-3,112 his6*) was used in this study. Yeast cells were cultured either in synthetic complete media supplemented with 2% dextrose or minimal media supplemented with essential amino acids and 0.1% [^{13}C]dextrose and 0.01% [^{15}N]ammonium sulfate. HU (Sigma-Aldrich) was added dry to a final concentration of 200 mM.

Flow cytometry. Cells were collected and mixed with 0.1% sodium azide in 0.2 M EDTA prior to fixing with 70% ethanol. Flow cytometry was performed as previously described (26) after staining cells with Sytox green (Molecular Probes). The data were analyzed with CellQuest software (Becton Dickinson).

Density transfer experiments. Dense-isotope substitution experiments were performed essentially as described earlier (24) with modifications to prepare samples for microarray analysis (31). After multiple generations of growth in medium in which the sole sources of carbon and nitrogen were isotopically dense (^{13}C, ^{15}N), cells were synchronized in G_1 by exposure to alpha mating pheromone. The culture was divided prior to filtering for transfer to isotopically light medium (^{12}C, ^{14}N) and synchronized at the G_1/S boundary by incubation at the restrictive temperature for the *cdc7-1* allele. One culture was treated with 200 mM HU during this block, while the other remained untreated. Unreplicated DNA (HH DNA) and replicated DNA (HL DNA) were separated by ultracentrifugation and separately labeled with cyanine-conjugated dUTP (GE Healthcare) as described by the Brown laboratory (http://cmgm.stanford.edu/pbrown/protocols/4_genomic.html). Samples were purified through a Sephadex column and collected by ethanol precipitation.

Microarray hybridization. The HH and HL fractions for each timed collection as described above were pooled separately to generate the samples for differential labeling and cohybridization to DNA microarrays (GEO platform accession number GPL1914; Fred Hutchinson Cancer Research Center). HH DNA labeled with Cy3-dUTP was cohybridized with HL DNA from the same timed sample labeled with Cy5-dUTP. Dye swaps were conducted concurrently to monitor for dye-specific effects. Hybridization values were extracted using GenePix 4.0 (Molecular Devices) and subjected to normalization and smoothing as defined in the materials and methods section of the supplemental material.

Control microarray. DNA from an untreated log-phase culture grown in complete (^{12}C, ^{14}N) medium was prepared identically to a density transfer sample (see above). Fractions that banded in the top 4.5% of the DNA in the gradient were pooled separately from the remainder of the genomic DNA. Microarray hybridization data of this DNA relative to the remaining genomic DNA were normalized and smoothed identically to those from the density transfer experiment.

Microarray data analysis. Data were normalized as described in the supplemental material and smoothed as described previously (30). Any data points in the most distal 12-kb window were excluded to avoid any artifacts introduced by the smoothing process near the chromosome ends (14).

Two-dimensional (2D) gel electrophoresis. High-molecular-weight DNA was isolated from cell pellets, digested with EcoRV, and subjected to electrophoresis in two dimensions (16). The fragments examined were as follows: *ARS305*, 4,206 bp; *ARS511*, 2,971 bp; *ARS1414*, 3,973 bp.

RESULTS

Extending the timeline. According to the current model of HU-induced replication stress, HU causes defects in both origin activation and fork progression. Forks are generated from early-firing origins, and, when low levels of dNTPs hinder these forks, late origins are actively repressed by the *MEC1*/*RAD53* checkpoint. These conclusions are based on examining replication for the first 90 to 120 min after adding HU to a synchronous culture of cells entering S phase. While this interval may be adequate for measuring the rate of nucleotide incorporation and fork movement, we felt that it might not be long enough to adequately distinguish between an inactivation of late origins and a delay in their initiation. We therefore extended the time frame over which samples of wild-type cells were collected after synchronously entering S phase in the presence of HU and monitored the genome for replication.

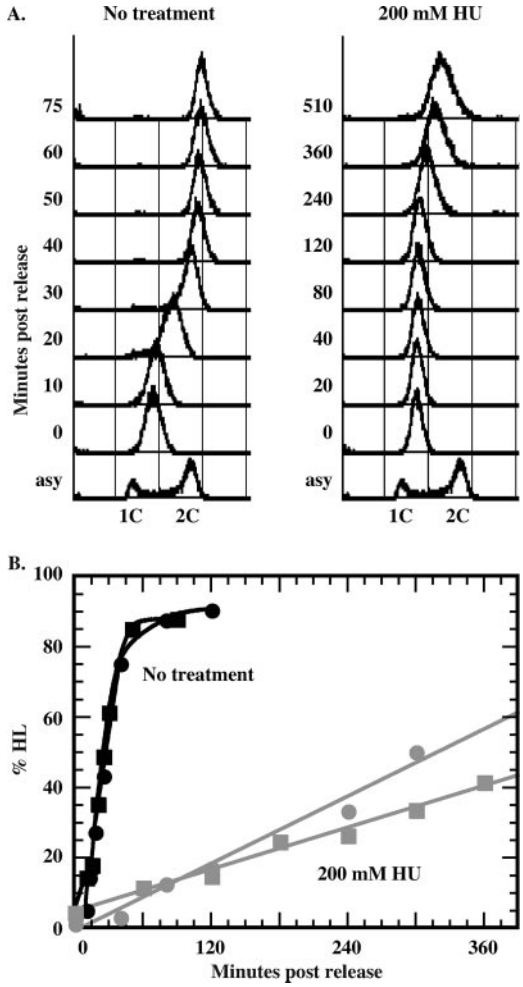

FIG. 1. HU dramatically slows S phase progression and DNA synthesis. Cells grown at 23°C in isotopically dense (^{13}C, ^{15}N) medium were synchronized by incubation with alpha mating pheromone. The cells were then filtered, resuspended in yeast complete (^{12}C, ^{14}N) medium and incubated for ~2 h at 37°C (the restrictive temperature for *cdc7-1*) with or without addition of HU. When 93% of the cells were budded, the culture was returned to 23°C to allow entry into S phase, and samples were collected periodically. (A) S phase progression in the absence (left) or presence (right) of 200 mM HU as measured by flow cytometry following staining with Sytox green. asy, asynchronous culture; 0 min, point at which cells were transferred back to 23°C. (B) DNA synthesis was quantified from the fractionated CsCl gradient samples by hybridizing slot blots with a probe made from total genomic DNA. The %HL at each sample time reveals the kinetics of genomic DNA synthesis from two independent collections (see text for details). Black symbols represent untreated samples; gray symbols represent HU-treated samples.

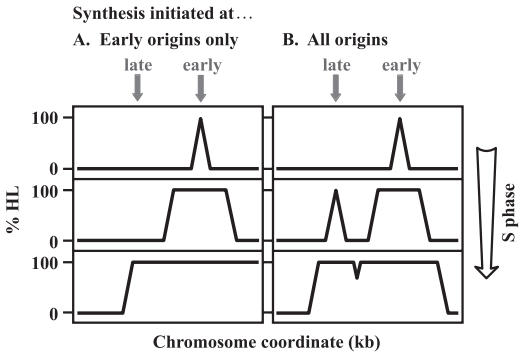

FIG. 2. Models for origin activation and S-phase progression in the presence of HU. Diagrams depict %HL replication profiles predicted for two different models. The filled arrows indicate positions of an early and a late origin. (A) Repression of late origin firing. The current intra-S phase replication checkpoint model predicts that early origins are activated while late origins are specifically inactivated. As S phase proceeds, late origins would eventually be replicated passively by slowly moving forks that emanated from early-firing origins. (B) Slowing of the S phase clock. The temporal program of origin activation is slow but intact. There is no specific repression of just late origins. As S phase begins, early origins are activated. Additional origins become active throughout S phase and are visualized by new zones of expanding synthesis. Note that the models are indistinguishable early in S phase (i.e., at low levels of net DNA synthesis).

Qualitatively, progression through S phase was assessed by flow cytometry. Cells were synchronized with alpha mating pheromone followed by incubation at the restrictive temperature for the *cdc7-1* allele. While the untreated culture attained 2C DNA content within 60 min of release from G_1 phase, the HU-treated culture was still in mid-S (~1.5C DNA content) as late as 510 min after the release (Fig. 1A). By 16 h in HU, cells reached a 2C DNA content and some of the cells divided to regenerate a 1C DNA peak (data not shown).

To quantify the extent of genome replication in HU-treated cells, we employed a modification of the Meselson/Stahl density transfer experiment (see Materials and Methods). Genomic DNA was isolated from samples collected at intervals throughout S phase, cut with a restriction endonuclease (EcoRI), and subjected to equilibrium centrifugation in gradients of CsCl. The gradients were fractionated and analyzed by slot blot hybridization with a whole-genome probe to quantify the percentage of the genome that had become hybrid in density (%HL DNA) in each timed sample (24). The resulting quantitative kinetic curves from two independent collections reveal that the extent of DNA synthesis is suppressed in the presence of HU to ~6% of untreated levels but that HL DNA nevertheless continues to increase for at least 6 h (Fig. 1B).

Replication profiles from microarray data. Since replication continues in HU, we wanted to ask whether additional origins were becoming active over time or whether all of the synthesis was due to extension of nascent strands from just the origins activated at the beginning of S phase. The predictions for these two models are illustrated in Fig. 2; in both models we expect to be able to detect moving forks, as, over time in S phase, they create expanding zones of HL DNA along the chromosome in both directions outward from each activated origin. If only early origins are able to initiate synthesis, then regions containing late origins would be passively replicated by these early forks (Fig. 2A) and not create new foci of expanding forks that appear later during the incubation (Fig. 2B).

To examine the kinetics of origin activation on a genome-wide scale, we isolated the HH and HL fractions from sequential samples collected during a density transfer experiment. We differentially labeled with fluorescent dyes the HH and HL DNA pools from each sample and cohybridized these to DNA microarrays (see Materials and Methods). Plotting %HL values against chromosomal coordinates gives an indication of the

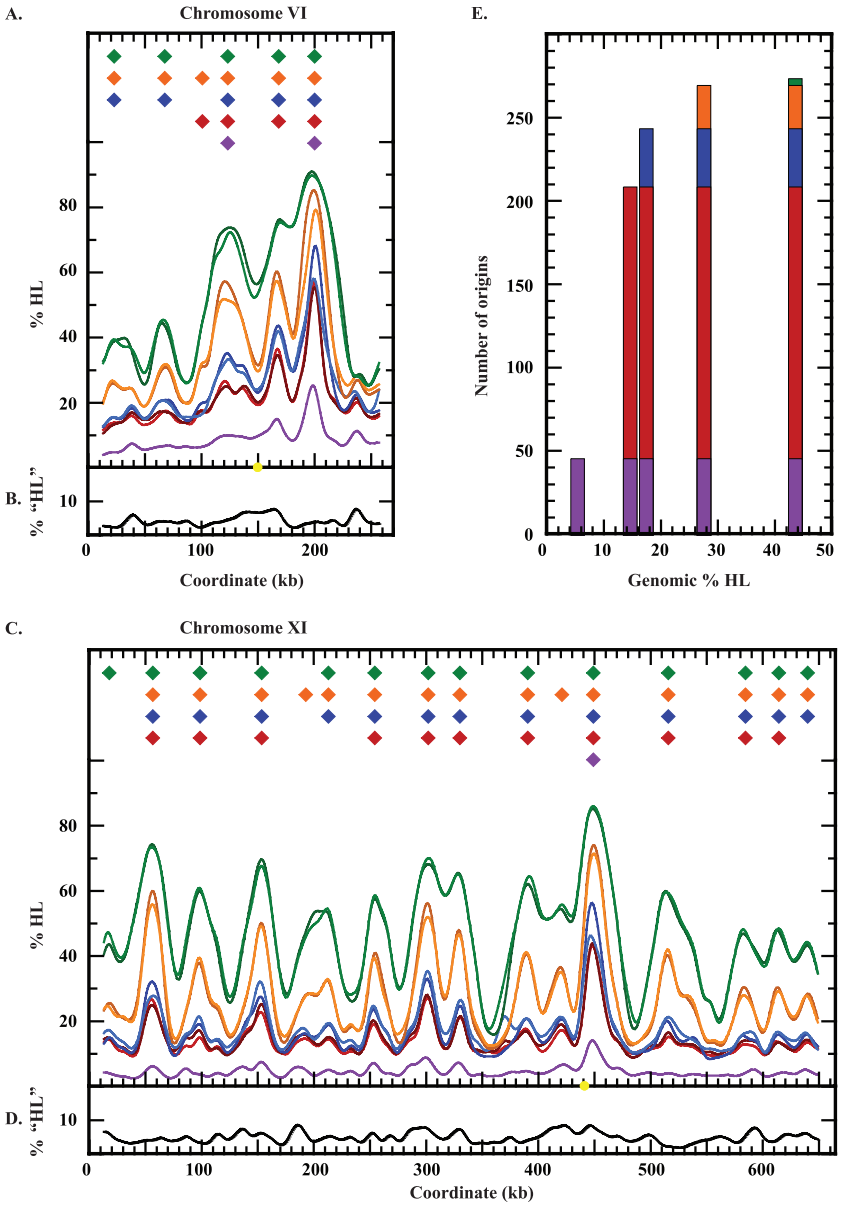

FIG. 3. Replication dynamics in the absence of HU. (A and C) Replication profiles for chromosomes VI and XI, respectively. Cells were grown and S phase samples were collected as described for Fig. 1. HH and HL DNAs from each timed sample were differentially labeled and cohybridized to microarray slides. The bottom panels show the accumulation of HL DNA at 10 (purple), 12.5 (red), 15 (blue), 17.5 (gold), and 25 (green) minutes postrelease plotted against chromosomal coordinate. Like colors indicate dye swaps, the yellow circle identifies the centromere. The top panels indicate the sample time(s) and locations at which origin activity (peaks in the chromosome profiles) was detected. See text for details on peak detection. (B and D) Control for HH contamination of HL DNA. DNA from logarithmically growing cells was subjected to centrifugation in a CsCl gradient. The "lightest" 4.5% of the DNA (analogous to HL DNA) was pooled separately from the remaining DNA. The DNAs were differentially labeled and cohybridized to a microarray. The data (%"HL," i.e., percentage of DNA present in the lighter pool) were plotted against chromosomal coordinates. This profile reveals those HH regions of the genome that are likely to contaminate the HL region of a gradient from density transfer samples. These data were also used to generate a baseline for identifying significant maxima in the density transfer experiment. See text for details. (E) Cumulative origin count during S phase plotted as a function of the percentage of the genome that is hybrid in density. The data are summed from the genome-wide profiles found in Fig. S1 and Table S1 in the supplemental material, with each origin color coded to identify the time at which activation of the origin was first identified in a significant fraction of cells in the culture.

relative extents of replication across the genome in any one sample. The normalized profiles for chromosomes VI and XI are presented in the bottom portions of Fig. 3A and C, respectively (see Fig. S1 in the supplemental material for the remaining chromosomes, Table S1 in the supplemental material for raw data, and materials and methods in the supplemental data for normalization details). Every local maximum is a potential origin of replication, and its time of appearance as a peak reflects the time at which that origin first became active in some fraction of the cells in the population. Over time, forks move away from origins into the neighboring regions, eventually filling in the valleys (termini) as forks from adjacent origins

meet (for example, see the termini at kb ~180 in Fig. 3A and kb ~75 in Fig. 3C). It is quite easy to identify early origins—those that have already fired in a substantial proportion of cells by 10 min into S phase—such as those at kb 199 in Fig. 3A (*ARS607*) and kb 448 in Fig. 3C (*ARS1114.5*). Late origins, such as *ARS603* at kb 67 in Fig. 3A, do not gain prominence as a maximum until later in S phase. Other minor peaks, such as the peak at kb 237 on chromosome VI (Fig. 3A), are present throughout the time course but never gain much prominence. From this kind of variability, two questions arise: what metric can we apply to distinguish when during S phase a peak becomes significant and which peaks are, in fact, origins?

To identify true origins and to determine at what time origin activity can first be detected, we created a computational tool to assess the significance of every peak in each sample. While peaks are presumptive origins, we needed an objective set of criteria to identify active origins and to match their locations in each sample over the time course. The Meselson/Stahl experiment relies on a CsCl gradient to physically separate HH and HL DNA. However, the position of a DNA fragment in a CsCl gradient is also affected by both its size and A+T content: the smaller the fragment, the broader the distribution in the gradient; the higher the A+T content, the less dense the fragment. Therefore, the HL portion of a given sample may be contaminated by small and/or A+T-rich sequences that are actually HH in nature. To obtain a baseline for the effects of these properties of various genomic EcoRI fragments on the replication profiles, we performed a control experiment that consisted of EcoRI-restricted genomic DNA from a culture grown in light medium that was fractionated in CsCl (see Materials and Methods). As there was no density substitution in this experiment, the only DNA to be found preferentially in the lighter portion of the gradient would be EcoRI fragments of small size or high A+T content. The DNA from this gradient was pooled in such a way as to mimic the distribution of HH and HL DNA in the replication experiment. The "HH" and "HL" portions of this control gradient were cohybridized to an array and normalized as described above. The profile of %"HL" (Fig. 3B and D; see Table S2 in the supplemental material) reveals those HH DNA sequences that potentially contaminate the HL portion of the CsCl gradients from the density transfer experiments and contribute to artificial peaks in the replication profiles. The control profile of chromosome VI (Fig. 3B) clearly explains the persistent maximum at kb 237 (which does not correspond to a known origin) and calls into question the significance of other maxima, such as the one at kb 37.

To systematically scan the genome for the presence of spurious maxima, we used the variance of these control data to define a significance baseline for the microarray data from the replication experiment. In each timed sample, the amplitude of each local maximum above its two flanking local minima was quantified and expressed as the number of standard deviations relative to the control. A clustering algorithm defined within a small window the average coordinate at which a significant local maximum was located across all samples in a time course. This coordinate was used as the identity for that peak to facilitate comparisons between data sets. We then asked whether the control data contained a local maximum within the window used to define the peak and subtracted its standard deviation value from that of the defined peak at each time point, in each data set. We required that a local maximum, to be considered significant, must have attained at least 2 standard deviations above the standard deviations calculated for the control at that chromosomal location. By this method, we defined 274 origins in the normal S phase (see Table S3 in the supplemental material), reflecting ~85% of the origins from a consolidated list taken from three previous studies, using a 6-kb window to match coordinates between data sets (4, 31, 37). Moreover, ~86% of the origins identified in this study were also defined by the ssDNA mapping technique (14).

To determine when in S phase each origin first becomes active, we identified the time at which each origin first attained significant amplitude relative to the surrounding loci (Fig. 3A and C, top). Plotting the cumulative number of activated origins against genomic %HL reveals a pattern of activation across S phase in which most origins can be detected by the time the genome has reached ~25% replicated, with very few new origin sites detected after this point (Fig. 3E).

Replication in HU. To explore the genomic pattern of origin activation in the presence of HU, we split a G_1-arrested culture into two equal portions. One portion was used to generate the data shown in Fig. 3. To the second portion we added HU (to a final concentration of 200 mM) 45 min before returning the culture to the permissive temperature for the *cdc7-1* allele. Upon release from the *cdc7-1* arrest and at timed intervals over the next 300 min, culture samples were harvested and the DNA was prepared for microarray analysis as described above. When comparing the replication profiles produced at the same absolute time after release into S phase (40 min; Fig. 4A), we saw an extreme difference in both the extent of replication and the particular origins that have been fired. We can clearly see that HU is having an effect at late origins, as there are no significant maxima at any of the late activated origins (such as *ARS603*) in the 40-minute treated sample. Qualitatively, this kind of difference has been reported by other investigators and is the basis of the argument that there is a specific failure to activate late origins in the presence of HU (33). What has not been noted in previous studies is that early origins are also being inhibited. If early origins were truly unaffected, the regions containing origins such as *ARS606* and *ARS607* should have accumulated the same high levels of HL DNA as are found in the untreated control sample (>90% HL at 40 min).

The replication profile for the 40-min HU sample actually looks comparable to the profile of the 10-min sample from the untreated culture (Fig. 4B): two culture samples with very similar total genomic %HL (3.2% versus 5.2%, respectively). Two later samples that have matching values for their genomic %HL (17.2%) are the 15-min untreated and the 120-min treated samples. Again, the HU-treated and untreated profiles look remarkably similar (Fig. 4C). To quantify the degree of similarity between these data, we used four metrics: %HL error analysis genome wide, %HL error analysis open reading frame (ORF)-by-ORF, singular-value decomposition, and derivative analysis of smoothed profiles (see materials and methods in the supplemental data for details). In no case did we observe any significant differences between the HU-treated

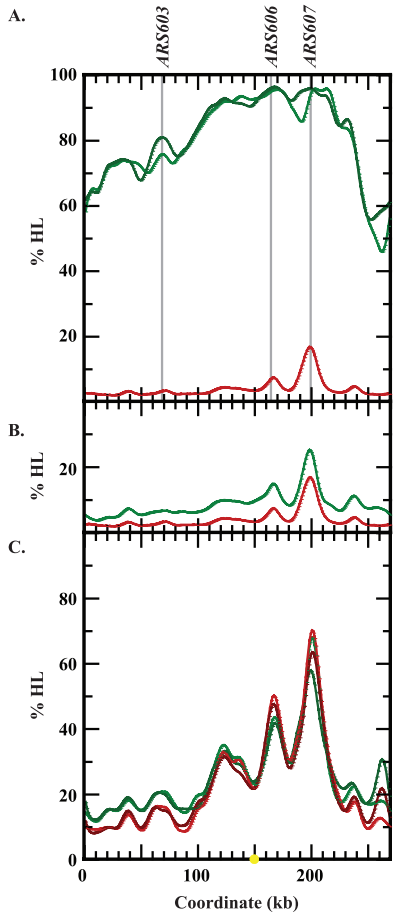

FIG. 4. Comparison of HU-treated and untreated samples. One-half of the synchronous culture used to generate the replication profiles in Fig. 3 and Fig. S1 in the supplemental material was treated with 200 mM HU and released into S phase as described in the text. Culture samples were collected periodically for 300 min, and the DNA was separated into HH and HL fractions in CsCl gradients. Replication profiles were generated as described for Fig. 3. (A) Chromosome VI replication profiles from HU-treated (red) and untreated (green) samples at the same absolute time in S phase (40 min after return to 23°C). (B and C) Chromosome VI replication profiles from HU-treated and untreated samples at times in S phase when the percent HL values of genomic DNA for untreated and treated sample were similar. (B) The 40-min HU-treated sample (red; 3.2%HL) is plotted with the 10-min untreated sample (green; 5.2%HL). (C) The 120-min HU-treated sample (red; 17.2%HL) is plotted with the 15-min untreated sample (green; 17.2% HL). See materials and methods in the supplemental material for statistical analysis used to compare the panel C samples.

and untreated data for any large set of contiguous ORF coordinates.

When the chromosome profiles from the HU-treated samples are arranged as a temporal series, we see a progression that is qualitatively very similar to that of the untreated S phase profiles although the time course in HU is much longer (Fig. 5A and C; see Fig. S2 and Table S4 in the supplemental material), indicating that fork rates are proportionally slowed across the genome. The profiles from the HU-treated S phase samples were subjected to the same analyses as the profiles from the untreated sample: identification of local maxima, determination of the significance of the local maxima over the background control (Fig. 5A and C, top; see Fig. S2 in the supplemental material), estimation of the time during the S phase that a peak attained significance, and correlation of peak positions with known origins. A total of 289 origins met all of these criteria (see Table S5 in the supplemental material); ~82% of the consolidated list of previously identified origins were identified in this data set (4, 31, 37), as well as ~90% of the origins in the untreated control from this study. Origins were categorized with respect to the sample in which they became significant, and the cumulative number of origins active in each sample is plotted in Fig. 5E. These data are consistent with the conclusions made for the origin activation program in the absence of HU (Fig. 3): origin activations are staggered over time, with few new origins becoming active after the genome reaches ~25% replication. We conclude from the results that the checkpoint that responds to HU does not appear to specifically distinguish between early and late activated origins. Instead, all origins are affected by the checkpoint since early origins are still becoming active in the majority of the population long after a normal S phase would have been completed. The S phase in HU appears to run in slow motion. In addition to the previously described pronounced decrease in the rate of fork movement (33), the overall tempo of origin activations is slowed by the presence of HU.

2D gel analysis. To verify that the local maxima we identified in the microarray analysis of HU-treated cells reflected bona fide initiation events and to measure origin activity over time, we used 2D gel electrophoresis to examine the structure of replication intermediates formed at a small subset of origins. Initiation generates bubble-shaped intermediates that are easily distinguished from other structures such as simple- or double-Y replication intermediates and recombination intermediates. We performed 2D gel analysis on pooled samples collected over two large time intervals from a synchronized culture released into S phase in the presence of HU. Comparison of bubble structures between the samples allows us to look for changes in the level of initiation during the two S phase intervals. Samples were pooled to represent "early" S phase (10 to 90 min after release) and "later" S phase (120 to 360 min). DNA was prepared as described previously (16) and analyzed by 2D gel electrophoresis and hybridization to various known origins with different replication times (T_{rep}) (Fig. 6A). These T_{rep} values were determined from slot blot hybridization (17, 31) and refer to the times at which origins have attained their half-maximal levels of replication in the population (25). Quantification of bubble structures (bubble/1N) from these 2D gels reveals a pattern of activation in which origins with earlier T_{rep} values have a greater proportion of bubbles in the early S phase pool (Fig. 6B). As the T_{rep} value increases, there is a shift in the bubbles into the later S phase pool (Fig. 6B). This result is consistent with the microarray data, confirming that origins continue to fire throughout S phase in the presence of HU according to an extended temporal program while maintaining the relative order of origin firing.

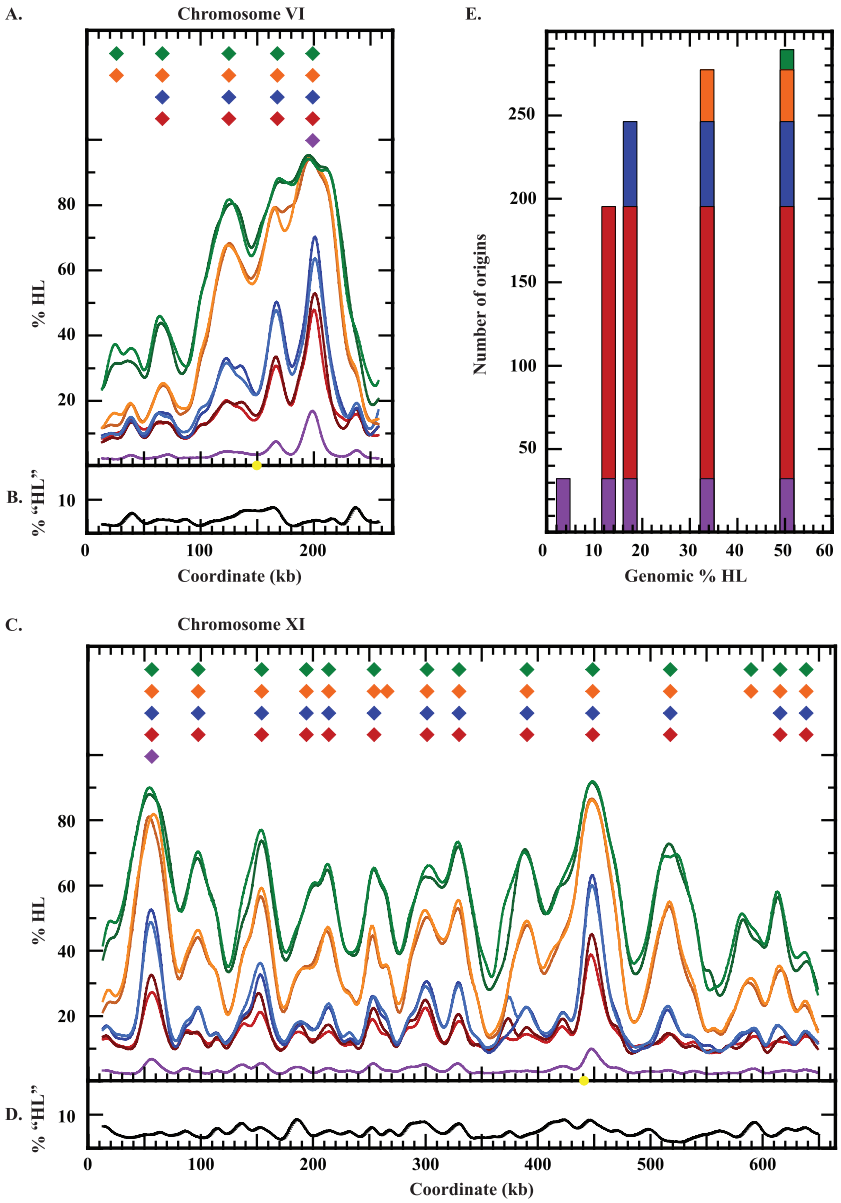

FIG. 5. Replication dynamics in the presence of HU. (A and C) Replication profiles for chromosomes VI and XI, respectively. The synchronous culture was treated with HU as described for Fig. 4 and in the text. Chromosome profiles and significant origin peaks were identified as described for Fig. 3 and in the text. The bottom panels show the accumulation of HL DNA at 40 (purple), 80 (red), 120 (blue), 240 (gold), and 300 (green) minutes postrelease plotted against the chromosomal coordinate. The yellow circle identifies the centromere. The top panels indicate the sample time(s) at which replication origins (peaks in the chromosome profile) are active. (B and D) Control experiment as described for Fig. 3. (E) Cumulative origin count during S phase is plotted as a function of the percentage of the genome that is hybrid in density. See the Fig. 3 legend for details.

DISCUSSION

Redefining the temporal program of origin activation. In earlier studies, we have reported the time of origin activation as a T_{rep} value: the time at which one-half of the cells in the culture have replicated that particular origin. While origins were classified as being "early" or "late," in actuality the temporal program is more of a continuum, with origin activation occurring over much of S phase. In our genome-wide analysis of the kinetics of replication in a normal S phase, we have not measured the T_{rep} values but have defined new criteria that allow us to detect the time in S phase when an origin is first recognized as being active and use it as an indicator of the temporal program of origin activation. Thus, although few new origins are detected after ~25% of the genome is replicated, the T_{rep} value for many origins will be later in S phase. It is still the case that origins are staggered in their time of activation and that the program is, in general, reproducible from cell to cell; however, "late," with respect to origin activation, is a relative term and need not imply the end of S phase.

This kinetic study of a normal S phase and the quantitative

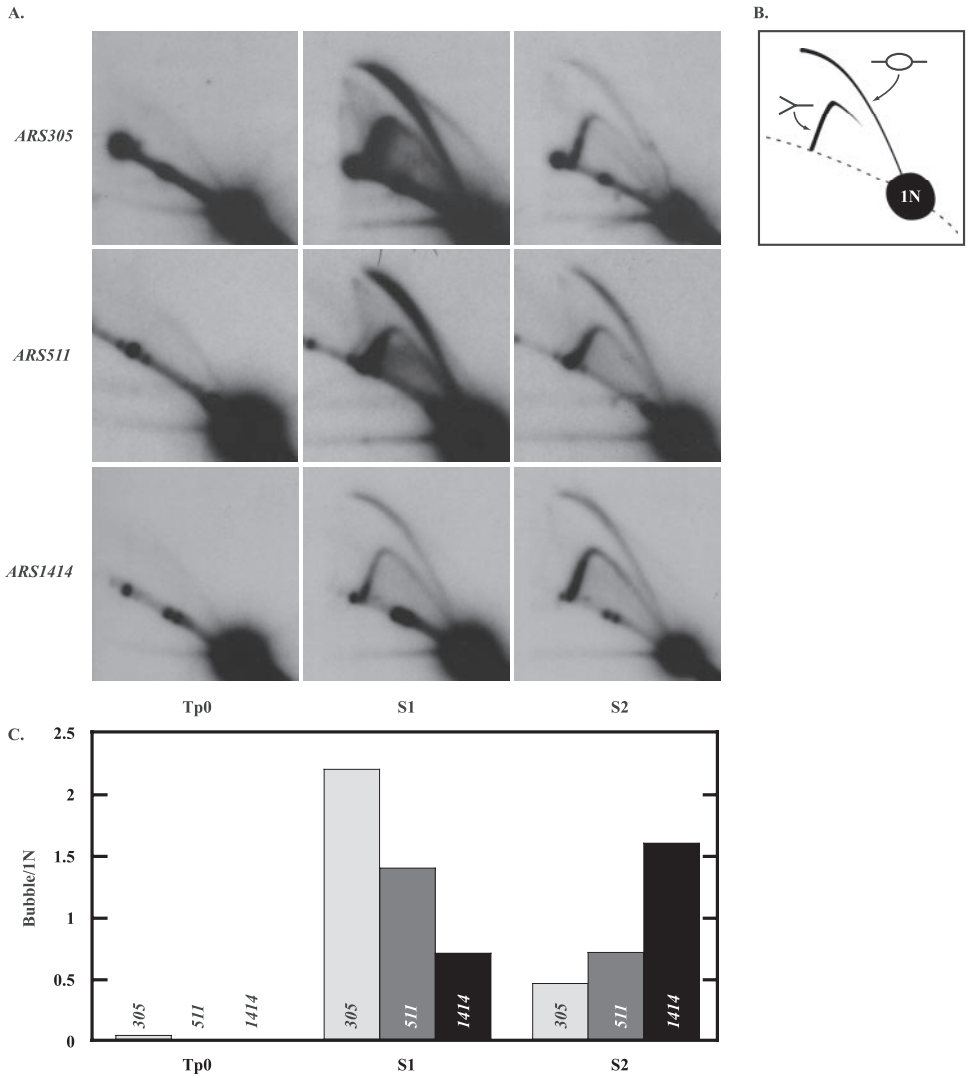

FIG. 6. 2D agarose gel analysis of origin activity in the presence of 200 mM HU. (A) Cells were grown in complete medium and synchronized with alpha mating pheromone followed by incubation at 37°C, the restrictive temperature for *cdc7-1*. Cells were allowed to enter S phase in the presence of 200 mM HU. Equal culture volumes were collected at designated intervals to create two pooled samples for 2D gel analysis. Pool S1 consisted of samples taken every 10 min from 10 to 90 min, inclusive. Pool S2 consisted of samples collected every 30 min from 120 to 360 min, inclusive. Tp0 refers to control cells harvested before release into S phase. High-molecular-weight DNA was isolated from each pool, digested with EcoRV, and subjected to electrophoresis in two dimensions (16). A Southern blot was probed sequentially to reveal replication bubbles at three different origins. Autoradiographs reveal replication intermediates at an early origin, *ARS305* (T_{rep} = 12.6 min), a mid-S origin, *ARS511* (T_{rep} = 18.7 min), and a late origin, *ARS1414* (T_{rep} = 24.7 min). (B) Cartoon illustrating the structures visualized by 2D gel electrophoresis. (C) Abundance of the bubble intermediates relative to the 1N spot of linear DNA for the three origins: *ARS305* (light gray), *ARS511* (medium gray), and *ARS1414* (black).

assessments of the replication profiles refine the distinction between time of activation and efficiency of activation. In our earlier density transfer experiments that examined pooled S phase samples, peaks of low amplitude could be explained by either late activation or early, but inefficient, activation (31). In our current study, we have imposed a limit on what we consider a significant peak and have defined the sampling time at which the peak achieves significance as its time of activation. However, despite the apparently remarkable synchrony we can achieve with the α-factor/*cdc7* arrest protocol (Fig. 1A), there is still significant asynchrony in origin activation, even with respect to the earliest origins. For example, at 10 min into a normal S phase, only a small fraction of cells have fired *ARS607*. Over the next 15 min, the fraction of cells steadily increases to reach 90%. We would argue that this behavior is consistent with that of a very efficient and early origin even though activation times are spread in the population over 20 min. Other origins aren't detected in the first 10 to 15 min but appear as significant peaks only later. The same spread in origin firing time may be true for these later-firing origins; however, the analysis of these origins is complicated by the fact that forks may be arriving from neighboring, earlier-activated origins. At present, we do not know whether the breadth of origin activation times for a given origin reflects the general asynchrony in the start of S phase among the population of cells or whether all cells release synchronously into S phase but

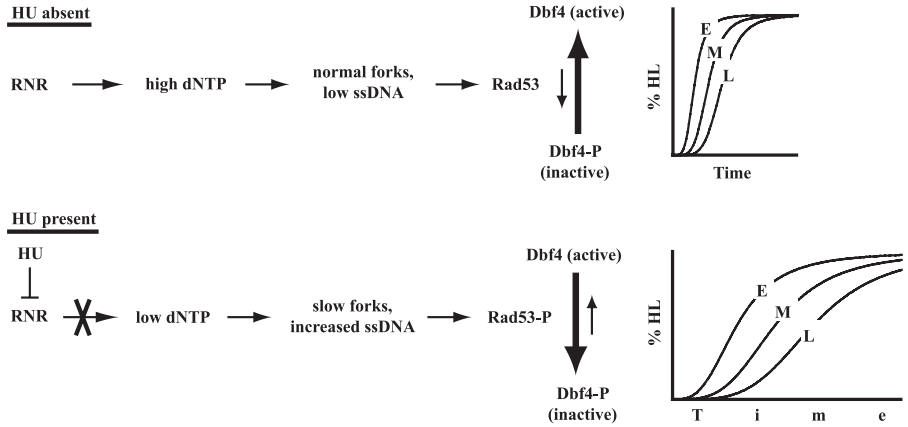

FIG. 7. Model for checkpoint-mediated modulation of the S phase clock. HU prevents the expansion of dNTP pools that would normally occur as cells enter S phase. As a result, cells entering S phase in the presence of HU show reduced fork migration rates and increased regions of ssDNA at the forks, eliciting the S phase checkpoint and the phosphorylation of Rad53 (34). Activated Rad53 in turn phosphorylates several proteins including Dbf4, the regulatory partner that together with Cdc7 comprises the DDK, the essential kinase needed at every origin for activation. The phosphorylated Dbf4 dissociates from Cdc7 (11, 12), and the resulting drop in the concentration of active DDK decreases the probability of origin activations, thereby stretching the program of origin activation.

there is variability in the precise order in which origins are activated within different cells in the population. Distinguishing between these two possibilities would require a method of analyzing single-cell replication kinetics—something that single-DNA molecule analysis could accomplish (29).

Replication in the presence of HU. The most striking finding in our experiment with HU is that the program of origin activation, the choice and order in which origins fire, appears indistinguishable from that in the absence of HU. This result is consistent with the observation that, in *S. pombe*, S phase progression continues in the presence of HU as nuclear replication foci appear, move, and fuse as they do in untreated cells, but over an extended time frame (25). In essence, we find that there is little difference in the overall number or identities of origins utilized in the presence or absence of HU when comparing samples that have achieved similar extents of replication. Of the 287 origins that were identified in the combined (treated and untreated) data sets, 220 (~77%) were common between the two data sets. However, this estimate is conservative as most of the origins that were scored in just one data set or the other actually had peaks at the corresponding location in the other data set (19 of 26 untreated origins and 31 of 41 treated origins) but were excluded because of our stringent scoring criteria.

HU-induced replication stress affects both elongation and origin initiation. The reduction in the rate of elongation makes sense in light of the reduced ability to produce dNTPs through the inhibition of ribonucleotide reductase by HU. In our experiments, the overall kinetics of genome replication (Fig. 1B) and the slow accumulation of HL DNA in termination regions (compare kb ~80 in Fig. 4A [40 min, untreated] and Fig. 5B [300 min, HU treated]) are consistent with a drastic slowing of replication forks, as described by Sogo et al. (34). Other studies have reported an inability to detect replication intermediates from late-replicating regions, including the late origin *ARS501* and the nonorigin sequence R11, compared to the early and efficient origin *ARS305* from wild-type cells released into HU (1, 33). Because replication intermediates were detected at *ARS501* by 90 min in both the *rad53* and *mec1* mutants, it appeared that the *MEC1*/*RAD53* checkpoint pathway specifically and actively repressed late origins in the presence of HU while allowing activation of early S phase origins. Our study sheds additional light on these previous studies and suggests a different mechanism for how the checkpoint responds to HU-induced replication stress: that rather than specifically inhibiting one temporal class of origins, the checkpoint acts to slow down the S-phase clock so that activations from all origins are delayed. The data reveal that the activity of every origin, from earliest to latest, is affected by the presence of HU and that attaining the same level of activity in the absence of HU as in its presence requires a significantly longer amount of time.

The link between limiting levels of nucleotides and the pace of origin firing is not direct. Low levels of nucleotides hinder fork progression from activated origins, and the ssDNA that forms at these forks elicits the S phase checkpoint response and the phosphorylation of Rad53. In this active state, the Rad53 kinase triggers several downstream events to regulate DNA synthesis. In one set of events, it promotes dNTP production by upregulating RNR activity (7, 13, 19, 38–40). However, because HU directly affects RNR activity by scavenging the tyrosyl-free radical in the active site of the enzyme, the dNTP pool remains limiting.

In addition to the effects on RNR, active Rad53 alters the phosphorylation state of many other proteins involved in replication and repair including the DNA polymerase α/primase complex, the single-strand DNA binding protein RPA, and Dbf4, the regulatory subunit of the Cdc7 kinase DDK (*D*bf4-*d*ependent *k*inase) (6, 30, 41). Phosphorylated Dbf4 dissociates from Cdc7, attenuating the kinase activity and causing its release from the origin recognition complex (12). Reduction in active DDK could have a direct effect on replication initiation at unfired origins since DDK is required throughout S phase to promote a late step in origin activation (5, 10). One candidate for this step in initiation is the recruitment of Cdc45p (and subsequently DNA polymerases), which has been shown to be DDK dependent (3).

Previously, this inactivation of DDK has been proposed as the mechanism for preventing late origins from firing in the presence of HU (11). In light of our finding that origin activations continue, albeit at a reduced tempo, in the presence of HU, we propose a revised version of that model (Fig. 7): rather than an all-or-nothing effect on DDK activity and hence on origin firing, Rad53 modulates DDK activity in proportion to the severity of the impediment to fork progression. As the concentration of active DDK drops, the intervals between subsequent initiation events at all unfired origins across the genome could become greater, thereby extending the replication program. If DDK were inactivated or reduced in activity during an otherwise normal S phase, forks moving outward from earlier-firing origins would passively replicate unfired origins. In the presence of HU, however, the rate of fork movement is slowed, presenting these later-firing origins with the opportunity to become activated. We imagine that the unknown factors that establish the temporal program are still present and direct the limiting amounts of active DDK to origins in their normal order (27). Limiting the pace at which new origins are activated would ensure that the low level of dNTPs could be funneled to a limited number of active forks, maintaining a slow but steady duplication of the genome. In the absence of Rad53, neither the upregulation of RNR nor the dissociation of DDK would occur and the origin firing program would occur at its normal pace, leading to a much larger number of activated origins without a sufficient supply of nucleotides to sustain fork progression.

ACKNOWLEDGMENTS

We thank the Fangman/Brewer/Raghuraman laboratory members, past and present, for support and helpful discussions. We are grateful to Wenyi Feng and Kim Lindstrom for critical review of the manuscript and to Dan Butler for valuable insight in designing the origin analysis tool used in the study. We also thank the crew at the FHCRC Genomics Facility for technical assistance. G.M.A. is especially grateful to Walt Fangman for his time spent as her mentor.

This work was supported by NIGMS grant 18926 to W. L. Fangman, B.J.B. and M.K.R.

REFERENCES

1. **Alcasabas, A. A., A. J. Osborn, J. Bachant, F. Hu, P. J. Werler, K. Bousset, K. Furuya, J. F. Diffley, A. M. Carr, and S. J. Elledge.** 2001. Mrc1 transduces signals of DNA replication stress to activate Rad53. Nat. Cell Biol. **3:**958–965.
2. **Allen, J. B., Z. Zhou, W. Siede, E. C. Friedberg, and S. J. Elledge.** 1994. The SAD1/RAD53 protein kinase controls multiple checkpoints and DNA damage-induced transcription in yeast. Genes Dev. **8:**2401–2415.
3. **Aparicio, O. M., A. M. Stout, and S. P. Bell.** 1999. Differential assembly of Cdc45p and DNA polymerases at early and late origins of DNA replication. Proc. Natl. Acad. Sci. USA **96:**9130–9135.
4. **Aparicio, O. M., D. M. Weinstein, and S. P. Bell.** 1997. Components and dynamics of DNA replication complexes in *S. cerevisiae*: redistribution of MCM proteins and Cdc45p during S phase. Cell **91:**59–69.
5. **Bousset, K., and J. F. Diffley.** 1998. The Cdc7 protein kinase is required for origin firing during S phase. Genes Dev. **12:**480–490.
6. **Brush, G. S., D. M. Morrow, P. Hieter, and T. J. Kelly.** 1996. The ATM homologue MEC1 is required for phosphorylation of replication protein A in yeast. Proc. Natl. Acad. Sci. USA **93:**15075–15080.
7. **Chabes, A., V. Domkin, and L. Thelander.** 1999. Yeast Sml1, a protein inhibitor of ribonucleotide reductase. J. Biol. Chem. **274:**36679–36683.
8. **Chabes, A., B. Georgieva, V. Domkin, X. Zhao, R. Rothstein, and L. Thelander.** 2003. Survival of DNA damage in yeast directly depends on increased dNTP levels allowed by relaxed feedback inhibition of ribonucleotide reductase. Cell **112:**391–401.
9. **Desany, B. A., A. A. Alcasabas, J. B. Bachant, and S. J. Elledge.** 1998. Recovery from DNA replicational stress is the essential function of the S-phase checkpoint pathway Genes Dev. **12:**2956–2970.
10. **Donaldson, A. D., W. L. Fangman, and B. J. Brewer.** 1998. Cdc7 is required throughout the yeast S phase to activate replication origins. Genes Dev. **12:**491–501.
11. **Duncker, B. P., and G. W. Brown.** 2003. Cdc7 kinases (DDKs) and checkpoint responses: lessons from two yeasts. Mutat. Res. **532:**21–27.
12. **Duncker, B. P., K. Shimada, M. Tsai-Pflugfelder, P. Pasero, and S. M. Gasser.** 2002. An N-terminal domain of Dbf4p mediates interaction with both origin recognition complex (ORC) and Rad53p and can deregulate late origin firing. Proc. Natl. Acad. Sci. USA **99:**16087–16092.
13. **Elledge, S. J., Z. Zhou, J. B. Allen, and T. A. Navas.** 1993. DNA damage and cell cycle regulation of ribonucleotide reductase. Bioessays **15:**333–339.
14. **Feng, W., D. Collingwood, M. E. Boeck, L. A. Fox, G. M. Alvino, W. L. Fangman, M. K. Raghuraman, and B. J. Brewer.** 2006. Genomic mapping of single-stranded DNA in hydroxyurea-challenged yeasts identifies origins of replication Nat. Cell Biol. **8:**148–155.
15. **Foiani, M., A. Pellicioli, M. Lopes, C. Lucca, M. Ferrari, G. Liberi, M. Muzi Falconi, and P. Plevani.** 2000. DNA damage checkpoints and DNA replication controls in *Saccharomyces cerevisiae*. Mutat. Res. **451:**187–196.
16. **Friedman, K. L., and B. J. Brewer.** 1995. Analysis of replication intermediates by two-dimensional agarose gel electrophoresis. Methods Enzymol. **262:**613–627.
17. **Friedman, K. L., J. D. Diller, B. M. Ferguson, S. V. Nyland, B. J. Brewer, and W. L. Fangman.** 1996. Multiple determinants controlling activation of yeast replication origins late in S phase. Genes Dev. **10:**1595–1607.
18. **Gasch, A. P., M. Huang, S. Metzner, D. Botstein, S. J. Elledge, and P. O. Brown.** 2001. Genomic expression responses to DNA-damaging agents and the regulatory role of the yeast ATR homolog. Mec1p. Mol. Biol. Cell **12:**2987–3003.
19. **Huang, M., and S. J. Elledge.** 1997. Identification of RNR4, encoding a second essential small subunit of ribonucleotide reductase in *Saccharomyces cerevisiae*. Mol. Cell. Biol. **17:**6105–6113.
20. **Huang, M., Z. Zhou, and S. J. Elledge.** 1998. The DNA replication and damage checkpoint pathways induce transcription by inhibition of the Crt1 repressor. Cell **94:**595–605.
21. **Koc, A., L. J. Wheeler, C. K. Mathews, and G. F. Merrill.** 2004. Hydroxyurea arrests DNA replication by a mechanism that preserves basal dNTP pools. J. Biol. Chem. **279:**223–230.
22. **Koc, A., L. J. Wheeler, C. K. Mathews, and G. F. Merrill.** 2003. Replication-independent MCB gene induction and deoxyribonucleotide accumulation at G_1/S in *Saccharomyces cerevisiae*. J. Biol. Chem. **278:**9345–9352.
23. **Lopes, M., C. Cotta-Ramusino, A. Pellicioli, G. Liberi, P. Plevani, M. Muzi-Falconi, C. S. Newlon, and M. Foiani.** 2001. The DNA replication checkpoint response stabilizes stalled replication forks. Nature **412:**557–561.
24. **McCarroll, R. M., and W. L. Fangman.** 1988. Time of replication of yeast centromeres and telomeres. Cell **54:**505–513.
25. **Meister, P., A. Taddei, A. Ponti, G. Baldacci, and S. M. Gasser.** 2007. Replication foci dynamics: replication patterns are modulated by S-phase checkpoint kinases in fission yeast. EMBO J. **26:**1315–1326.
26. **Newlon, C. S., L. R. Lipchitz, I. Collins, A. Deshpande, R. J. Devenish, R. P. Green, H. L. Klein, T. G. Palzkill, R. B. Ren, S. Synn, et al.** 1991. Analysis of a circular derivative of *Saccharomyces cerevisiae* chromosome III: a physical map and identification and location of ARS elements. Genetics **129:**343–357.
27. **Nougarede, R., F. Della Seta, P. Zarzov, and E. Schwob.** 2000. Hierarchy of S-phase-promoting factors: yeast Dbf4-Cdc7 kinase requires prior S-phase cyclin-dependent kinase activation. Mol. Cell. Biol. **20:**3795–3806.
28. **Nyberg, K. A., R. J. Michelson, C. W. Putnam, and T. A. Weinert.** 2002. Toward maintaining the genome: DNA damage and replication checkpoints. Annu. Rev. Genet. **36:**617–656.
29. **Pasero, P., A. Bensimon, and E. Schwob.** 2002. Single-molecule analysis reveals clustering and epigenetic regulation of replication origins at the yeast rDNA locus. Genes Dev. **16:**2479–2484.
30. **Pellicioli, A., C. Lucca, G. Liberi, F. Marini, M. Lopes, P. Plevani, A. Romano, P. P. Di Fiore, and M. Foiani.** 1999. Activation of Rad53 kinase in response to DNA damage and its effect in modulating phosphorylation of the lagging strand DNA polymerase. EMBO J. **18:**6561–6572.
31. **Raghuraman, M. K., E. A. Winzeler, D. Collingwood, S. Hunt, L. Wodicka, A. Conway, D. J. Lockhart, R. W. Davis, B. J. Brewer, and W. L. Fangman.** 2001. Replication dynamics of the yeast genome. Science **294:**115–121.
32. **Rivin, C. J., and W. L. Fangman.** 1980. Replication fork rate and origin activation during the S phase of *Saccharomyces cerevisiae*. J. Cell Biol. **85:**108–115.
33. **Santocanale, C., and J. F. Diffley.** 1998. A Mec1- and Rad53-dependent checkpoint controls late-firing origins of DNA replication. Nature **395:**615–618.
34. **Sogo, J. M., M. Lopes, and M. Foiani.** 2002. Fork reversal and ssDNA accumulation at stalled replication forks owing to checkpoint defects. Science **297:**599–602.
35. **Tercero, J. A., and J. F. Diffley.** 2001. Regulation of DNA replication fork progression through damaged DNA by the Mec1/Rad53 checkpoint. Nature **412:**553–557.
36. **Weinert, T. A., G. L. Kiser, and L. H. Hartwell.** 1994. Mitotic checkpoint genes in budding yeast and the dependence of mitosis on DNA replication and repair. Genes Dev. **8:**652–665.
37. **Yabuki, N., H. Terashima, and K. Kitada.** 2002. Mapping of early firing origins on a replication profile of budding yeast. Genes Cells **7:**781–789.
38. **Yao, R., Z. Zhang, X. An, B. Bucci, D. L. Perlstein, J. Stubbe, and M. Huang.**

2003. Subcellular localization of yeast ribonucleotide reductase regulated by the DNA replication and damage checkpoint pathways. Proc. Natl. Acad. Sci. USA **100:**6628–6633.

39. **Zhao, X., E. G. Muller, and R. Rothstein.** 1998. A suppressor of two essential checkpoint genes identifies a novel protein that negatively affects dNTP pools. Mol. Cell **2:**329–340.
40. **Zhou, Z., and S. J. Elledge.** 1993. DUN1 encodes a protein kinase that controls the DNA damage response in yeast. Cell **75:**1119–1127.
41. **Zou, L., and B. Stillman.** 2000. Assembly of a complex containing Cdc45p, replication protein A, and Mcm2p at replication origins controlled by S-phase cyclin-dependent kinases and Cdc7p-Dbf4p kinase. Mol. Cell. Biol. **20:**3086–3096.